

Oil-dispersal modelling: re-analysis of the Rena oil spill using open-source modelling tools

Hannah F. E. Jones^{1,2}, Martin T.S. Poot², Julia C. Mullarney², Willem P. de Lange², Karin R. Bryan^{2*}

¹Present Address: Waikato Regional Council, Private Bag 3038, Hamilton, New Zealand

²Coastal Marine Group, School of Science, University of Waikato, Hamilton, New Zealand.

*Corresponding author: K. R. Bryan

Tel:

Email: kbryan@waikato.ac.nz

Key words: oil spill response, Tauranga Harbour, Gnome, Bay of Plenty, wind climate

Abstract (150 words)

Oil spill forecast modelling is typically used immediately following a spill to predict oil dispersal and promote mobilisation of more effective response operations. The aim of this work was to map oil dispersal following the grounding of the container ship “Rena” on Astrolabe reef and to verify the results against observations. Model predictions were broadly consistent with observed distribution of oil contamination. However, some hot spots of oil accumulation likely due to surf-zone and rip-current circulation were not well represented. Additionally, the model was run with 81 differing wind conditions to show that the events occurring during the grounding represented the typical likely behaviour of an oil spill on Astrolabe Reef. Oil dispersal was highly dependent on prevailing wind patterns, and more accurate prediction would require better observations of local wind patterns. However, comparison of predictions with observations indicated that the GNOME model was an effective low-cost approach.

Keywords:

Oil spill, hazard, Gnome, probability, wind event, ship grounding

Introduction

On the 5th of October, 2011, the 47,000 tonne container ship “Rena” ran aground on the Astrolabe Reef (37.540°S 176.425°E) on the approach to Tauranga Harbour (Figure 1). There were 1,733 tonnes of oil on board the Rena, of which 1,300 tonnes were recovered before May 4th 2012 (source:

35 Maritime NZ). During the week after the grounding, approximately 350 tonnes of heavy fuel oil were
36 released onto the shelf, where the oil was subjected to tidal currents, wind-induced currents, and
37 shelf currents, both of which advected and dispersed the oil, with a large fraction stranding on Waihi
38 Beach, Matakana Island, Mount Maunganui Beach, Papamoa Beach, and lesser amounts being
39 dispersed farther afield. A small fraction entered Tauranga Harbour and Maketu Estuary.

40

41 A number of institutions provided oil-spill response forecast modelling immediately following the
42 Rena grounding to guide response operations. However, there was no formal quantitative
43 verification of the predictions provided by the models; accurate predictions require careful model
44 calibration and verification against observations of both currents, and oil dispersal and shoreline
45 accumulation; and the necessary data were not available during the response. The aim of this study
46 was to use freely-available open-source modelling tools to hindcast the oil dispersal following the
47 Rena grounding, to verify the results against information on oil accumulation collected by Maritime
48 New Zealand, and to use multiple model simulations to provide a preliminary hazard map, from
49 which an understanding of most common oil dispersal patterns associated with a grounding on
50 Astrolabe Reef can be inferred. The advantage of open-source modelling systems is that there is a
51 greater likelihood of multiple institutions using the same systems, and so model set-up files and
52 results can be easily exchanged between working groups, allowing for greater collaboration,
53 verification and quality-control.

54

55 **Methods**

56 Astrolabe Reef is approximately 7 km north of Motiti Island and 24 km northeast of Mt. Maunganui
57 in the Bay of Plenty in the North Island of New Zealand (Figure 1). The Bay of Plenty coastline is a
58 low-energy wave environment, sheltered from the prevailing westerly and south-westerly swell that
59 affects other areas of New Zealand (Heath, 1985; Gorman et al., 2003). Tides (at Tauranga) range
60 between 1.62 m for spring tides and 1.24 m for neap tides. The tidal currents on the shelf are
61 relatively weak ($0.05\text{-}0.10\text{ m}\cdot\text{s}^{-1}$), compared to wind-driven currents that reach $0.25\text{ m}\cdot\text{s}^{-1}$ (Black et
62 al., 2005; Longdill et al., 2010).

63

64 Delft3D-FLOW, developed by Deltares (the Netherlands) and available as open-source software, is a
65 hydrodynamic simulation program that calculates non-steady flow from tidal and meteorological
66 forcing on a rectilinear or curvilinear boundary fitted grid. Delft3D-FLOW may be implemented in 3D,
67 with the vertical grid defined using the sigma (σ) co-ordinate approach, or in 2D using a depth-

68 averaged approach (2DH) (Deltares 2011). The model has been extensively validated (e.g. Elias et al.
69 2000; Lesser et al. 2004).

70

71 In this study, the Delft3D model domain included both the northern and southern basins of Tauranga
72 harbour. The grid extended approximately 25 km offshore (to a water depth of around 70 – 90 m)
73 and approximately 60 km along shore from Waihi to Maketu. The grid resolution was 200 x 200 m in
74 the horizontal and the grid was rotated at an angle of 50° to the North-South axis (Figure 2).

75 Bathymetry was derived from various sources, such as echo-soundings and nautical charts (Kwoll,
76 2010). The model was run in both 3D and 2D simulation modes. The 3D mode provided slightly more
77 accurate results around the entrance to Tauranga Harbour, and so was used to simulate conditions
78 around the 05/10/2011 event. The 2D model was used to run 81 different scenarios that were used
79 to assess the likely impact of spills occurring during other wind conditions. The 2D version was used
80 for this rather than the 3D version because the minor difference in modelled open coast flow fields
81 did not warrant the order of magnitude-larger run-times associated with the 3D model. The number
82 and thickness of the layers in the 3D model were determined based on the need for fine resolution
83 near the bed (to resolve the logarithmic profile of the horizontal velocity components in the vertical)
84 and near the surface. Based on these considerations (and the need for the layer thickness to have a
85 smooth distribution) the 3D model had 16 σ -layers, with layer thicknesses between the bed and the
86 surface set to 1.5, 2, 2.8, 4, 5.6, 7.8, 11, 15.3, 15.3, 11, 7.8, 5.6, 4, 2.8, 2, and 1.5 % of total depth.

87

88 Hydrodynamic simulations were forced at the open boundaries using the tidal constituents M2, N2,
89 S2, K1, MU2, O1, and L2. Time series of water levels at the four corners of the open boundaries
90 were derived from water levels predicted by the NIWA tidal model

91 (<http://www.niwa.co.nz/services/online-services/tide-forecaster>), which also includes these
92 constituents. Constituents were extracted from the water levels using the tidal harmonic analysis
93 package, “t_tide” (Pawlowicz et al. 2002). Flow at the boundaries was forced using astronomic

94 Riemann boundary conditions (3D model) or Neuman conditions (depth-averaged model) at the
95 open boundaries. Riemann boundary conditions are based on a linearised Riemann invariant (F_R ; m s⁻¹):

97

$$F_R = U + \eta \sqrt{\frac{g}{h}},$$

100 where, U is velocity, η is sea surface elevation, g is acceleration due to gravity, and h is water depth.

101 This type of boundary reduces reflection of obliquely incident waves and is non-reflective for

102 outgoing waves normal to the boundary (e.g. Mullarney et al., 2008). Free slip (no shear stress)
103 conditions were applied at the closed boundaries, and the vertical velocity profile at the boundaries
104 was a logarithmic function of the water depth.

105

106 *Delft3D calibration and validation methods*

107 The Delft3D-FLOW calibration simulation began on 1st October 2011 from a “cold start” (i.e. uniform
108 water levels, no currents) and ran for 30 days with a 60 s time step (3D model) and 15 s time step
109 (2D model). To reduce numerical instabilities in the initial adjustment period, the boundary forcing
110 was gradually applied over a smoothing period. Continuous measurements of tidal elevation were
111 provided by Bay of Plenty Regional Council and Port of Tauranga for three stations inside the
112 harbour, Omokoroa, Sulphur Point and Tug Berth, and one station outside of the harbour, A Beacon
113 (Figure 2). ADCP current meter data collected in the harbour entrance were also provided by Port of
114 Tauranga. The model was calibrated by adjusting parameters including the Chézy roughness
115 coefficient, threshold depth, and horizontal eddy viscosity. The model error was represented by
116 model performance statistics; the coefficient of determination (R^2) and the mean absolute error
117 (MAE). Model calibration is shown for the 3D version, and similar results were obtained for the 2D
118 version.

119

120 Parameters resulting from the Delft3D model calibration were fixed for a further month-long
121 simulation for the purposes of model validation. Water level and current data collected at five sites
122 inside and outside the harbour between 10th May and 10th June 2006, described in detail in Spiers
123 et al. (2009), were used for model validation. Tidal elevation, current velocity and direction were
124 measured at three sites outside (C1, C2 and C3) and one site inside (C5) Tauranga Harbour (Figure 2).
125 Station C4 was not used as it was found to contain erroneous data (Spiers et al., 2009).

126

127 *Delft3D model calibration results*

128 The Delft3D models were calibrated by adjusting the bottom roughness coefficient, threshold depth,
129 and horizontal eddy viscosity (Table 1). The final calibrated 3D-Chézy coefficient was spatially
130 variable, ranging from 80-40 $m^{1/2} s^{-1}$ for the 3D model and 180-10 $m^{1/2} s^{-1}$ for the 2D model from
131 shallow and deep water, corresponding to a roughness length (z_0) that increased with depth from
132 approximately 0.0001 m and 0.0053 m for the 3D model. These values of z_0 are consistent with those
133 provided in the literature, for un-rippled mud/sand and rippled sand (e.g. Soulsby 1997).

134

135 The Delft3D modelled and measured water levels for the stations used in model calibration and
136 validation were in good agreement for both models (R^2 0.96 – 0.98, MAE 0.07 – 0.08 m; results for
137 the 3D model are provided in Table A1.1 and Figure 3 (thin dashed line, 3D model, thin solid line, 2D
138 model). The models predicted tidal amplitudes to within 0.03 m and predicted tidal phases for the
139 major tidal constituents (M2, N2 and S2) at sites outside Tauranga harbour and near the harbour
140 entrance to within 5 degrees. However, the models tended to under-predict the phase in the inner
141 harbour (i.e. at Omokoroa) by approximately 6 - 7 degrees (Table A1.1).

142

143 For the calibration period, 3D modelled current velocities for the Delft3D model were consistently
144 lower than those measured at the Port of Tauranga ADCP site (MAE 0.41 m s⁻¹; Table A1.2; Figure 3).
145 This was particularly true for the 2D model. However, the model did capture the pattern of higher
146 ebb tide velocities, compared to flood, and modelled current directions compared well with
147 measured data (MAE 18 degrees for flood tide, and 30 degrees for the ebb).

148

149 Velocities at validation sites C1, C2 and C3 were also consistently lower than measured velocities
150 (MAE 0.04 to 0.10 m s⁻¹, 52 to 67 % of the average measured current velocity), but were better
151 predicted at site C5 (MAE 0.10 m s⁻¹, 22 % of the average measured current velocity; Table A1.2;
152 Figure 3). The current velocity MAE in the 2D version was lower than that of the 3D model both
153 outside and inside the harbour, whereas the 3D version had lower MAE for flows around the
154 complex entrance area. As with the ADCP (calibration) site, the models captured the pattern of
155 higher ebb tide velocities at sites inside and near the harbour entrance (i.e. C2, C3 and C5; Table
156 A1.2). Modelled current direction compared very well with measured data at site C5 (MAE ebb tide
157 3.5 degrees and MAE flood tide 12.8 degrees for the 3D model (with a slightly better fit for the 2D
158 model, Figure 3), with reasonable agreement between measured and modelled data for sites C1, C2
159 and C3 (MAE approximately 10 – 14 degrees for the 3D model and slightly more for the 2D model).
160 Note that the calibration and verification sites were not established specifically for the purposes of
161 this study, and are clustered around the entrance, where the tidal currents are likely to be higher. It
162 is possible that calibration/validation would not be as successful using observations in deeper water
163 where shelf currents may be more important.

164

165 *GNOME calibration and validation methods*

166 GNOME (General NOAA Oil Modeling Environment) is a freely-available oil spill trajectory model that
167 simulates the movement of oil due to winds, surface currents and spreading (NOAA 2012). The spill
168 trajectory includes both a “best guess” and a “minimum regret” solution that takes into account the

169 uncertainty in the model inputs. GNOME is a two-dimensional Eulerian/Lagrangian model that
170 requires three major inputs: maps, movers (current, wind or diffusion) and spills. The movement of
171 the oil is calculated from the u (east-west) and v (north-south) velocity components, summed for all
172 the movers at each time step, using a 1st-order Runge-Kutta method.

173

174 For this study, output from Delft3D for 5th October (i.e. when the Rena grounded) to 30th October
175 2011 was used as input in GNOME as a current mover. Currently, GNOME can only use 2D currents,
176 so in the case where the 3D model was used, surface flows from the Delft3D model output were
177 used as input to GNOME. Maps for the Western Bay of Plenty coastline were obtained from the
178 GOODS (GNOME Online Oceanographic Data Server) map generator tool
179 (<http://gnome.orr.noaa.gov/goods>). Hourly wind speed and direction were acquired from NIWA's
180 CliFlo service (National Institute of Water and Atmospheric Research National Climate database,
181 <http://cliflow.niwa.co.nz>) and applied spatially uniformly over the entire domain.

182

183 GNOME calculates diffusion of the oil (random spreading) using a simple random walk based on a
184 diffusion value (representing horizontal eddy diffusivity, and ranging from 0.1 m² s⁻¹ to 100 m² s⁻¹).
185 Oil spills can be modelled as up to 10,000 Lagrangian Elements (LEs), each of which have parameters
186 assigned including location, release time, age, pollutant type, and status (floating, beached,
187 evaporated or off the map). Windage is the movement of oil by the wind, which is typically about 3%
188 of the wind speed (NOAA, 2012). Refloating in GNOME is determined by the refloat half-life, which is
189 defined as the number of hours in which half of the oil that has beached is removed by an offshore
190 wind, diffusion or raised water levels (such as an incoming tide). Additional parameters describe
191 uncertainty in the wind, current and diffusion movers, and thus control the output for the minimum
192 regret LEs.

193

194 In this study, the Rena spill was initialised using data from Maritime New Zealand that described the
195 timing and amount of oil spilled from the vessel. Some of these data consisted of estimates obtained
196 from mapping the approximate dimensions of the surface accumulation near the wreck from a
197 helicopter. The uncertainty surrounding the release behaviour of the oil is an unfortunate but
198 unavoidable limitation of this study (and represents a continuing challenge for modelling oil spills of
199 this type). The Rena grounded at 2:00 am on 5th October 2011 and approximately 350 tonnes of oil
200 leaked from the ship (typically at low tide) between then and late October. The majority of the oil
201 likely leaked from the vessel between 10th and 12th October, when weather conditions were poor
202 (winds speeds typically 5 – 8 m s⁻¹, from the north to north-easterly direction).

203

204 A verification database was collated from data on oil dispersal and accumulation following the Rena
205 grounding obtained from Maritime New Zealand in the form of SCAT (Shore Clean-up Assessment
206 Techniques) survey reports and over-flight observations. Data were extracted and compiled to
207 summarise critical information (where available), such as the survey/oil location, the beach zone
208 surveyed (e.g., lower, middle, or upper intertidal), the amount of oil observed (e.g., as percentage
209 cover on the shoreline), and oil character (e.g., tar balls, tar patties).

210

211 From the SCAT data, two metrics were calculated for each day in October following the grounding: i)
212 the average oil percentage cover (averaged across the intertidal zones for each location surveyed
213 and averaged across all locations surveyed) and ii) the maximum oil percentage cover. Data on the
214 quantity of oil removed from the beaches was insufficient to estimate the actual amount (in tonnes)
215 of oil accumulated on the shoreline, thus it was not possible to quantitatively compare GNOME
216 output (tonnes of oil accumulated on the shoreline) with SCAT data (percentage cover of oil on the
217 shoreline). However, GNOME output and SCAT data were compared to assess model accuracy with
218 respect to the timing and location of oil accumulation. Additionally, maps of oil dispersal (in the
219 water) and accumulation (on the shoreline) were provided by Maritime New Zealand that
220 summarised the SCAT and over-flight observations, which were compared with GNOME model
221 output.

222

223 The hazard associated with the Rena grounding was assessed by running 81 wind event scenarios
224 over 21 days covering a spring and neap tide. The 81 events were chosen from the range of wind
225 speeds and directions that were measured at Tauranga Airport from 1995 to 2012. Note that the
226 winds were maintained constant during the 3 week modelling period. (It was not possible to model
227 unsteady wind conditions and include all combinations that were statistically likely to occur).

228

229 *GNOME model calibration results*

230

231 The GNOME model was calibrated by adjusting parameters associated with diffusion, the refloat
232 half-life, model time step, uncertainty and windage (Table 2). The refloat half-life was set at 12 hours
233 for the shelf model to reflect the (predominantly) sandy beaches on the open coastline (Dancuk
234 2009). Along- and cross- current uncertainty values were increased (compared to default values) due
235 to the uncertainty around the current predictions by the Delft3D model.

236

237 The amount of oil released, floating, beached, evaporated and dispersed, and that which had moved
238 out of the modelled area (“off map”) was output from the model every 6 hours for the entire
239 simulation (Figure 4a). The majority of the oil over most of the simulation remained floating;
240 although a significant proportion (100 tonnes or approximately 35 % of that released) evaporated or
241 dispersed within a few days. The amount of oil beached on the shoreline averaged ~10 % of the total
242 released over the entire simulation (i.e. 5th – 30th October), although this peaked at 30 % at three
243 and ten days after release. By the end of the simulation ~40 % of the oil had travelled outside of the
244 modelled area (mostly to the north and east). The amount of oil entering Tauranga Harbour and
245 Maketu estuary was relatively small (< 5 - 10 tonnes).

246

247 **Results**

248

249 *Comparison of GNOME output with observations*

250 GNOME model output generally compared well with observations. The amount of oil beached across
251 the entire model domain (the best estimate, not including the uncertainty solution) was output
252 from the model every 6 hours and visually compared with SCAT report data (Figure 4b). The GNOME
253 model predicted that oil would first reach the shoreline on 11th October, and by 13th October large
254 amounts of oil (~ 60 – 90 tonnes) would have accumulated on the coastline. However, the model did
255 not predict the arrival of the small amount of oil which was observed to reach the shoreline on the
256 10th October. Although it was not possible to estimate the actual amount of oil that did accumulate
257 on the shoreline based on SCAT reports which gave estimates of percentage cover, the observations
258 do indicate that the maximum oiling did occur on the 13th October, as predicted by the model
259 (Figure 5). Further peaks in oil accumulation on 15 – 16th October and 19 – 20th October captured by
260 the model also largely matched observations of maximum and average oil coverage on the shoreline.

261

262 The GNOME model indicated that oil entered Tauranga harbour (through the southern entrance)
263 from a north-easterly direction between 10th and 13th October. The wind direction changed to north-
264 westerly from 13th to 14th October, and the majority of the oil began to move offshore. These model
265 results are consistent with SCAT surveys which indicated presence of oil inside Tauranga harbour by
266 17th October (Figure 4b).

267

268 *Preliminary hazard assessment*

269 Wind data from Tauranga Airport show that southwesterly winds, with wind speeds of between 4
270 and 8 m/s are the most common conditions around Tauranga (Figure 6 and Figure 7A). Of the most

271 common wind speeds, winds from 220 degrees were also associated with the longest arrival times of
272 oil at the shoreline. Northeasterly winds were the wind patterns which caused the modelled oil spill
273 to reach the coastline most quickly, with the largest wind events causing the fastest arrival times
274 (Figure 7B) (although the probability of the large wind events occurring was very low). Northeasterly
275 winds were associated with the great tonnage of accumulated oil at the shoreline over the 20 day
276 modelling period (Figure 7C).

277

278 **Discussion**

279 *GNOME model performance*

280 The GNOME model compared well with observations (i.e. SCAT surveys), generally predicting the
281 timing and location of oiling on the shoreline, peaks in oil accumulation, and timing of the oil entry
282 into Tauranga harbour. The qualitative nature of the observed data prevented quantitative
283 comparison between model output and observed oil accumulation. More accurate measurement of
284 the amount of oil that accumulated on shorelines could have improved GNOME model verification,
285 but was not a priority during Rena oil spill clean-up response operations.

286

287 There was a slight discrepancy between the timing of the first instance of oil on the shoreline (10th
288 October observed *cf.* 11th October modelled). However, there was uncertainty around the timing
289 and amount of oil lost from the vessel in the days following the grounding (Maritime New Zealand,
290 2011), and inaccurate initialisation of the oil spill in GNOME will affect the accuracy of the simulation
291 results. When used in real-time operations, (*i.e.* when used to forecast, rather than hindcast), the oil-
292 spill amount and extent can be initialised and updated based on over flight data (NOAA, 2012),
293 which should improve model predictions. The GNOME model appears to over-predict the oil
294 beached on 19th – 20th October, but SCAT reports indicate that there was beach clean-up (*i.e.*
295 removal of oil) in progress before and around this time. It was not possible to take removal of oil
296 from beaches into account with the GNOME model due to the uncertainty around the amount and
297 location of oil removed, which may account for the over-prediction of oiling around this time.

298

299 The oil that did beach on the shoreline was not evenly dispersed, with “hot spots” of accumulation
300 evident in the model output and in SCAT observations, for example, at Papamoa Beach, parts of the
301 western shoreline of Motiti Island, and Okurei Point (east of Maketu). Surf zone rip currents are
302 common along the sandy beaches of the Bay of Plenty coast (e.g. Stephens *et al.*, 1999), and these
303 can trap oil within their recirculation systems. SCAT observations indicate that the oiling along the
304 coastline from Mt. Maunganui to Maketu indeed had a patchy distribution. However, the model only

305 includes the effect of winds and tides, and does not include the effect of waves and surf-zone
306 currents, so was unable to resolve these finer scale features.

307

308 *Preliminary analysis of oil spill hazard*

309 The results from modelled scenarios indicate that the time taken for the first oil to reach the shore
310 varies between 14 hours and more than 20 days (Figure 7). Oil was found to only reach shore within
311 20 days if there were onshore winds, suggesting that even relatively weak wind-driven currents may
312 provide greater forcing for oil dispersal than tidal currents in the Bay of Plenty. To test the relative
313 importance of tidal currents to determining the hazard, the Gnome scenario modelling was also
314 undertaken without the tidal currents. Interestingly, tidal currents were found to have an important
315 effect, particular during periods with low onshore winds, causing the first arrival of oil at the Bay of
316 Plenty shoreline to occur at least 3 days earlier when tidal currents were included (Figure 7 D and E).

317

318 Scenarios of moderate-high (7-9 m/s) wind speeds from 340 degrees (NNW), (and including tidal
319 currents), had shorter times to first arrival at the shoreline compared with other onshore wind
320 scenarios of same wind speed due to some of the initial oil leaked being transported directly onto
321 Motiti Island rather than more typically around the island. The wind in early October 2011 varied in
322 direction (Figure 5A), and so the scenarios modelled in Figure 7 represent the most (onshore winds
323 only) and least (offshore winds only) hazardous end members. The case associated with the least
324 beached oil had weak (1 m/s) winds travelling nearly parallel to the shoreline (100 and 340 degrees
325 or ESE and NNW respectively) which had the effect of extending the plume alongshore. In the case
326 of higher wind speeds (11 m/s and greater) and a NNW wind, most of the beached oil on Motiti
327 Island was refloated on the leeward side, and hence only 91 metric tons was measured.

328

329 Figure 8 shows three different examples of predicted oil dispersal after the first six days following
330 the grounding of the Rena. In the scenario which was forced by the observed winds (panel A), there
331 were predominantly offshore winds forcing the oil plume away from the shore. A small amount of oil
332 from the initial leak reached the shore on the 10th October, consistent with observations (SCAT
333 surveys). Panels B and C show the most hazardous scenarios, which both involve strong (>11 m/s)
334 onshore (NNE) winds which forced the floating oil towards the Southern entrance of Tauranga
335 Harbour. All these scenarios show that the wind conditions that occurred during the Rena grounding
336 switched between typical wind conditions which were moderately hazardous, to the extremely low
337 hazard offshore wind conditions. The wind records show that direction switches every 2-4 days (as in

338 Figure 5) are typical of the wind climate around Tauranga. If the Rena grounding had occurred during
339 consistent and strong northwesterlies, the impact could have been much greater.

340

341 *Model performance*

342 The performance of both Delft3D models was generally satisfactory, with water levels, tidal
343 amplitude and phase predicted very well inside and outside of the harbour. Tidal phase tended to be
344 slightly under-predicted at the Omokoroa site in the inner harbour, but this discrepancy may be
345 partly owing to the location of the Omokoroa water level recorder in a small channel that was not
346 well represented in the Delft3D model grid (which had a resolution of 200 x 200m). There was
347 relatively little difference between the 2D and 3D model versions except right at the southern inlet
348 entrance, suggesting that stratification effects are likely not important at this time of the year. This
349 result may not have been the case if the spill had occurred during summer.

350

351 Although current velocity and direction were predicted well at some sites, the model performed less
352 well at predicting current velocity at and just outside of the southern Tauranga harbour entrance,
353 with velocity tending to be under-predicted at these sites. A model with a finer grid resolution
354 around Tauranga harbour entrance and tidal channels would likely improve the accuracy of the
355 predicted current velocities. A Delft3D model of the Tauranga Harbour southern entrance area
356 (Spiers et al. 2009) achieved a MAE of less than 20% of measured velocities (using the same dataset
357 as used for model validation in this study), by increasing grid resolution around the entrance to 2 x 2
358 m. However, such a reduction in grid size, (the model grid in the current study is 200 x 200 m),
359 requires a large reduction in the model time step, (3 seconds *cf.* 60 seconds in this study), which
360 leads to a large increase in model run times; simulations covering large areas and timespans are thus
361 rendered largely impractical. In future implementations, further consideration could be given to
362 using a variable grid resolution and more finely resolved bathymetry for areas near harbour
363 entrances, whilst retaining a coarser grid resolution offshore.

364

365 The Delft3D model was forced by tides only, so discrepancies between measured and modelled
366 velocities may be attributable to wind or swell conditions. However, preliminary simulations with
367 wind forcing included in the Delft3D model did not improve model fit, despite the inclusion in the
368 model of finely resolved vertical layers near the surface. Wind forcing was instead included in the
369 GNOME particle tracking model, which included additional parameters for windage and uncertainty,
370 and this inclusion led to improved predictions of oil dispersal and accumulation. The omission of
371 winds in Delft3D may be particularly relevant at sites away from the influence of harbour entrances

372 or tidal channels where tidal forcing may not be the major driver of current velocities, such as at site
373 C1. Although the Bay of Plenty coastline is a typically a low-energy wave environment (Heath 1985),
374 it is exposed to swell from the north and north-easterly direction that may affect surface currents.
375 Inclusion of, or coupling to, a wave model would increase the complexity (and run times) of the
376 hydrodynamic model, but may improve model performance. We note that GNOME considers only
377 surface oil dispersal and not the dispersal of tarballs and other oil-mineral aggregates that travel
378 deeper in the water column, and so predicted dispersal is particularly sensitive to surface wind
379 conditions. Modelling simulations also did not include shelf currents. It is possible that the relatively
380 enclosed geometry of the Bay of Plenty limited the effect of these kinds of currents, and it is likely
381 that performance would not have been so good if the spill had occurred in a much more open
382 location.

383

384 *Recommendations for oil spill modelling in relation to hazard management*

385 Available data for model calibration and validation comprised sites that were clustered around the
386 Tauranga Harbour southern entrance (Figure 2), as research and monitoring effort typically having
387 been focused on the Port and its entrance. However, the lack of available data for the wider shelf
388 hinders verification of model performance for areas away from Tauranga Harbour; collection of
389 further hydrodynamic data being outside the scope and resources of this study. This highlights the
390 scarcity of observational data in New Zealand waters that can be used to verify model predictions.
391 Oil-dispersal predictions may be highly uncertain if based on unverified hydrodynamic models.
392 Importantly, this study has highlighted the following critical areas for future research and
393 collaboration:

394

395 i) National operational oceanography capability could be improved by ensuring shelf modelling is
396 based on open-source models and freely (and easily) available observations so that uptake of
397 technology is maximised. If agreement were reached on a common open-source model so that
398 bathymetries and boundary files can easily be exchanged between working groups, resources could
399 be utilised much more effectively (in terms of both cost and predictive accuracy of the models), and
400 this would undoubtedly lead to improved hazard management. However, we note that using
401 multiple models to obtain similar results promotes higher levels of confidence in the modelling
402 outcomes.

403

404 ii) New Zealand has a scarcity of observational buoys in its waters. Such real time observations and
405 data assimilative models are imperative in order to make accurate real time modelling forecasts.

406 Such operational forecasts are needed in many situations, from oil spill response to monitoring of
407 harmful algal blooms to search and rescue operations. Furthermore, by including measurements
408 from all aspects of the marine environment, not only physical measurements but also
409 biogeochemical and optical water quality measurements, such buoys provide a window to longer-
410 term oceanic changes. Deployment of a number of buoys in key locations and free access to the
411 data would greatly enhance capability for marine environmental prediction. Deploying and
412 maintaining such an observational system is complex, costly and would require multi-organisational
413 cooperation between all interested parties such as government, regional councils, Crown Research
414 Institutes and Universities. Consideration should also be given to other monitoring systems, such as
415 HF RADAR which could be used for operational forecasting of currents around harbour entrances.
416 Such systems provide surface current patterns in real-time, over kilometre scales, which can be used
417 to train forecasting models to provide highly-accurate results.

418

419 **Conclusions**

420 The results of this study demonstrate that the use of open-source modelling software (specifically
421 the hydrodynamic model Delft3D and the particle tracking model GNOME) can be used as an
422 effective and relatively low-cost tool to predict oil dispersal. Qualitative comparison of model output
423 with observations of oil accumulation following the Rena grounding indicate the GNOME model
424 provided encouraging ability to predict the first arrival time, and the general levels of oil
425 accumulation along the Bay of Plenty coastline. This agreement may have been due, in part, to the
426 partially-enclosed nature of the Bay of Plenty, and modelling of a more open coast location might
427 need to include non-tidal non-wind driven (e.g. shelf currents). Multiple scenarios aimed at
428 understanding the likely hazard associated with an Astrolabe grounding highlight the important role
429 of wind strength and direction in determining the likely severity of the outcome. The orientation of
430 the Bay of Plenty coastline makes the area particularly susceptible to wind events from the
431 northeast.

432

433 This study also highlights critical limitations in current capabilities for oil-dispersal modelling in New
434 Zealand. For example, the lack of validation data for offshore currents and winds and the lack of a
435 common modelling framework (ideally open-source) for all institutes that are likely to be involved in
436 any early-response efforts. Such a common modelling system would allow the necessary model set
437 up parameters to be easily transferred between all working groups. This would allow resilience to
438 issues such as variations in capability of each working group which can vary with time owing to
439 personnel changes and absences. New Zealand has a disproportionately large coastal ocean to

440 manage with a small pool of science experts, and hence the ability to transfer knowledge and
441 resources quickly is the key to fast and efficient response times.

442

443 **Acknowledgements**

444 We acknowledge the support of Maritime New Zealand in providing access to data, and funding
445 from the Ministry for the Environment. Dr Christian Winter and Eva Kwooll from the University of
446 Bremen provided Delft3D model grids. Laura Hines collated the oil spill response information from
447 Maritime New Zealand, funded by the University of Waikato summer scholarship programme. Dr
448 Kyle Spiers provided water level and current meter data for around the entrance, and the Port of
449 Tauranga provided water level and current meter data. Bay of Plenty Regional Council provided
450 water level data from inside Tauranga Harbour.

451

452 **References**

- 453 Black, K.P., Beamsley, B., Longdill, P.C., and Moores, A., (2005). *Bay of Plenty current and*
454 *temperature measurements: aquaculture management areas, data report*. Report for Environment
455 Bay of Plenty, ASR Ltd, Raglan, New Zealand. 67 pp.
- 456 Dancuk, S.N., (2009) .*The fate and transport of light petroleum hydrocarbons in the lower Mississippi*
457 *River delta*. PhD Thesis, Louisiana State University.
- 458 Deltares (2011). Delft3D-FLOW: Simulation of multi-dimensional hydrodynamics flows and transport
459 phenomena, including sediments. *User manual version 3.15*. Deltares, The Netherlands.
- 460 Elias, E.P.L., Walstra, D.J.R., Roelvink, J.A., Stive, M.J.F., and Klein, M.D. (2000). Hydrodynamic
461 validation of Delft3D with field measurements at Egmond. In '27th International Conference on
462 Coastal Engineering', 2000, Sydney, Australia, pp. 2714-2727
- 463 Gorman, R.M., Bryan, K.R., and Laing, A.K., (2003). A wave hindcast for the New Zealand Region —
464 Nearshore validation and coastal wave climate, *New Zealand Journal of Marine and Freshwater*
465 *Research*, **37**, 567–588.
- 466 Heath, R.A. (1985). A review of the physical oceanography of the seas around New Zealand - 1982.
467 *New Zealand Journal of Marine and Freshwater Research* **19**(1), 79-124.
- 468 Kwohl, E. (2010). Evaluation of the Tauranga Harbour numerical model. MSc Thesis, University of
469 Bremen.
- 470 Lesser, G.R., Roelvink, J.A., van Kester, J.A.T.M., and Stelling, G.S. (2004). Development and
471 validation of a three-dimensional morphological model. *Coastal Engineering* **51**(8–9), 883-915.
- 472 Longdill, P. C., Healy, T.R., and Black. K.P., (2008). Transient Wind-driven Coastal Upwelling on a Shelf
473 with Varying Width and Orientation.*New Zealand Journal of Marine and Freshwater Research* **42** (2),
474 181–96. doi:10.1080/00288330809509947.
- 475 Maritime New Zealand (2011) Rena Grounding Timeline. Available at
476 <http://www.maritimenz.govt.nz/Rena/>, accessed on December 1st, 2014.
- 477 Mullarney, J.C., Hay, A.E., and Bowen, A.J. (2008). Resonant modulation of the flow in a tidal
478 channel. *Journal of Geophysical Research*, **113**(C10007). doi:10.1029/2007JC004522.
- 479 NOAA (2012). General NOAA Operational Modeling Environment (GNOME) Technical
480 Documentation. National Oceanic and Atmospheric Administration, Office of Response and
481 Restoration.
- 482 Pawlowicz, R., Beardsley, B., and Lentz, S. (2002). Classical tidal harmonic analysis including error
483 estimates in MATLAB using T-TIDE. *Computers & Geosciences* **28**(8), 929-937.
- 484 Soulsby, R. (1997) 'Dynamics of marine sands: A manual for practical applications.' (Thomas Telford
485 Publications Ltd.: London) 249 pp.

486 Spiers, K.C., Healy, T.R., and Winter, C. (2009). Ebb-jet dynamics and transient eddy formation at
 487 Tauranga harbour: Implications for entrance channel shoaling. *Journal of Coastal Research* **25**(1),
 488 234-247.

489 Stephens, S.A., Healy, T.R., Black, K.P., and de Lange, W.P. (1999). Arcuate duneline embayments,
 490 infragravity signals, rip currents and wave refraction at Waihi beach, New Zealand, *Journal of Coastal*
 491 *Research* **15**(3), 823-829.

492 **Tables**

493

494 **Table 1: Calibrated model parameters for the Delft3D models.**

Parameter	Value	Units
Threshold depth	0.01	m
Horizontal eddy viscosity	10	m ² s ⁻¹
Vertical eddy viscosity	0	m ² s ⁻¹
Turbulence model	k-ε	
Number of layers (3D)	16	
Number of layers (2D)	1	
Chézy roughness coefficient	Spatially variable (80 –	m ^{1/2} s ⁻¹
Chézy roughness coefficient	Spatially variable (180	m ^{1/2} s ⁻¹

495

496

497 **Table 2: Calibrated model parameters for the GNOME model**

498

Parameter	Value	Units
Diffusion	1	m ² s ⁻¹
Diffusion uncertainty	1	
Refloat half-life	12	Hours
Time step	0.17	Hours
Windage	1-4	%
Wind speed scale	2	m s ⁻¹
Wind angle scale	0.4	Radians
Along current uncertainty	25	%
Cross current uncertainty	25	%

499

500

501

502 **Figure Captions**

503 **Figure 1:** Tauranga harbour and Bay of Plenty coastline. Location of the Rena grounding, Astrolabe reef,
 504 marked with an asterisk.

505

506 **Figure 2:** Delft3D model grid and location of calibration (red star) and validation (green triangle) sites.

507

508 **Figure 3:** Measured and modelled water levels for validation sites C1 (A), C3(B), C2(D) and calibration site A
509 Beacon (C), and measured and modelled current velocity and direction for the calibration ADCP site (E) and
510 validation site C5 (F).

511

512 **Figure 4:** Panel A: Amount of oil released from the Rena, floating, beached on the shoreline, evaporated and
513 dispersed or “off map” (i.e. outside of modelled area) throughout the duration of the GNOME simulation (5th
514 October – 30th October 2011). Panel B: Modelled (GNOME) oil beached on the shoreline (in metric tons) and
515 maximum and average oil percentage coverage as assessed by SCAT surveys.

516

517 **Figure 5:** (a) Wind speed and direction measured at Tauranga airport in October 2011, with time of Rena
518 grounding indicated by the arrow. Positive values on y axis represent northerly winds, negative values
519 represent southerly winds. For example, offshore (southerly to south-westerly) winds are evident from 6th to
520 8th October 2011. (b) Modelled (GNOME) amount of oil beached on shoreline. Note peak in oil beached on
521 shoreline 12th to 13th October after a period of onshore (north-easterly) winds, followed by a reduction in oil
522 beached after moderate (> 5 m/s) offshore (southerly) winds.

523

524 **Figure 6:** Wind speeds and directions measured at Tauranga Airport from 1995 to 2012. The colorbar is wind
525 speed and the length of each radial bar reflects the probability of that wind condition occurring.

526

527 **Figure 7:** (A) The proportion of wind speeds and directions measured at Tauranga airport from 1995 to 2012,
528 split into 81 wind events. (B) Modelled (GNOME) times after the initial oil leak for the first oil to be beached,
529 for constant wind conditions. Simulations with no oil landing onshore within 20 days are labelled ‘>20D’. (C)
530 Modelled (GNOME) quantities of oil beached at twenty days after the initial oil leak, for constant wind
531 conditions. Circled in red are scenarios with (A) the most common wind condition, (B) the shortest time of
532 arrival, and (C) the largest quantity of beached oil. Maps of the circled scenarios in Panels B and C are shown in
533 Figure 8. Panels D and E are for the same wind conditions as in panels B and C, but have been modelled
534 without including the effect of tides.

535

536 **Figure 8:** Maps of modelled (GNOME) oil plumes on 11th October at 9:20pm NZST, six days after the initial oil
537 leak began, for (A) recorded wind conditions, (B) shortest time elapsed for first beaching of oil, and (C) largest
538 quantity of beached oil after twenty days. Black dots represent the best guess location of oil particles, while
539 red dots represent the minimum regret positions of oil particles.

540

Appendix 1

Table A1.1: Statistical comparison of measured and Delft3D modelled water levels, tidal amplitude and phase. R^2 is the coefficient of determination, and MAE is the mean absolute error.

Site	Calibration or Validation	Water levels		Tidal constituents									
		R^2	MAE (m)	M2 amp error (m)	M2 phase error (deg)	N2 amp error (m)	N2 phase error (deg)	S2 amp error (m)	S2 phase error (deg)	K1 amp error (m)	K1 phase error (deg)	O1 amp error (m)	O1 phase error (deg)
A Beacon	Calibration	0.982	0.072	-0.01	-1.42	-0.01	1.29	0.01	4.77	-0.01	3.67	-0.01	8.26
Tug Berth	Calibration	0.971	0.078	0.03	-5.64	0.01	-3.69	0.02	1.19	-0.01	0.39	-0.01	9.93
Sulphur Point	Calibration	0.974	0.082	-0.01	-4.53	-0.01	-3.82	0.03	-1.24	-0.01	-15.46	0.01	2.89
Omokoroa	Calibration	0.965	0.082	-0.01	-6.73	-0.01	-6.56	0.03	-6.36	-0.01	-14.68	0.01	17.02
C1	Validation	0.968	0.077	-0.04	-4.23	0.01	1.95	0.03	-0.28	-0.02	-11.77	0.01	13.48
C2	Validation	0.965	0.078	-0.03	-3.89	0.02	2.45	0.03	0.79	-0.02	-13.48	0.01	15.23
C3	Validation	0.965	0.077	-0.02	-4.25	0.02	1.91	0.03	-0.37	-0.02	-13.61	0.01	16.54
C5	Validation	0.958	0.082	0.00	-6.20	0.03	1.34	0.03	-2.45	-0.02	-14.42	0.01	16.61

Table A1.2: Statistical comparison of measured and modelled (Delft3D) current speed and direction. MAE is the mean absolute error, Mean_{obs} is the mean of the measurements and Mean_{mod} is the mean of the model output.

Site	Calibration or Validation	Tide	Speed (m s ⁻¹)			Direction (degrees)		
			Mean _{obs}	Mean _{mod}	MAE	Mean _{obs}	Mean _{mod}	MAE
ADCP	Calibration	Total	1.10	0.72	0.41			
		Flood	1.10	0.72	0.33	145.77	163.88	18.11
		Ebb	1.48	0.85	0.61	8.00	337.19	30.48
C1	Validation	Total	0.06	0.02	0.04			
		Flood	0.05	0.02	0.04	240.41	239.51	13.70
		Ebb	0.02	0.02	0.01	66.28	64.48	9.13
C2	Validation	Total	0.19	0.10	0.10			
		Flood	0.12	0.07	0.06	213.19	205.17	13.31
		Ebb	0.29	0.14	0.22	20.71	21.33	11.17
C3	Validation	Total	0.16	0.06	0.10			
		Flood	0.12	0.06	0.05	178.40	174.57	13.02
		Ebb	0.23	0.09	0.21	334.05	335.48	10.86
C5	Validation	Total	0.45	0.41	0.10			
		Flood	0.47	0.35	0.10	278.54	265.47	12.82
		Ebb	0.55	0.50	0.08	88.02	87.11	3.52

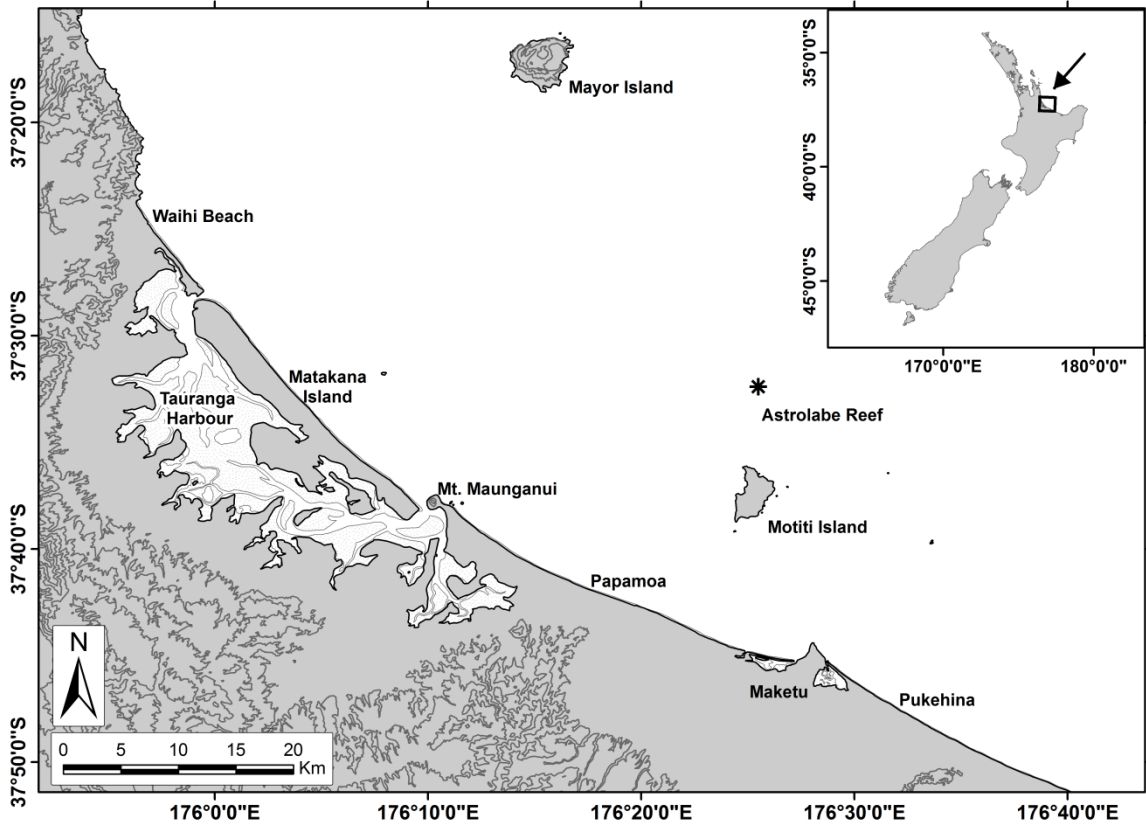


Figure 1: Tauranga harbour and Bay of Plenty coastline. Location of the Rena grounding, Astrolabe reef, marked with an asterisk.

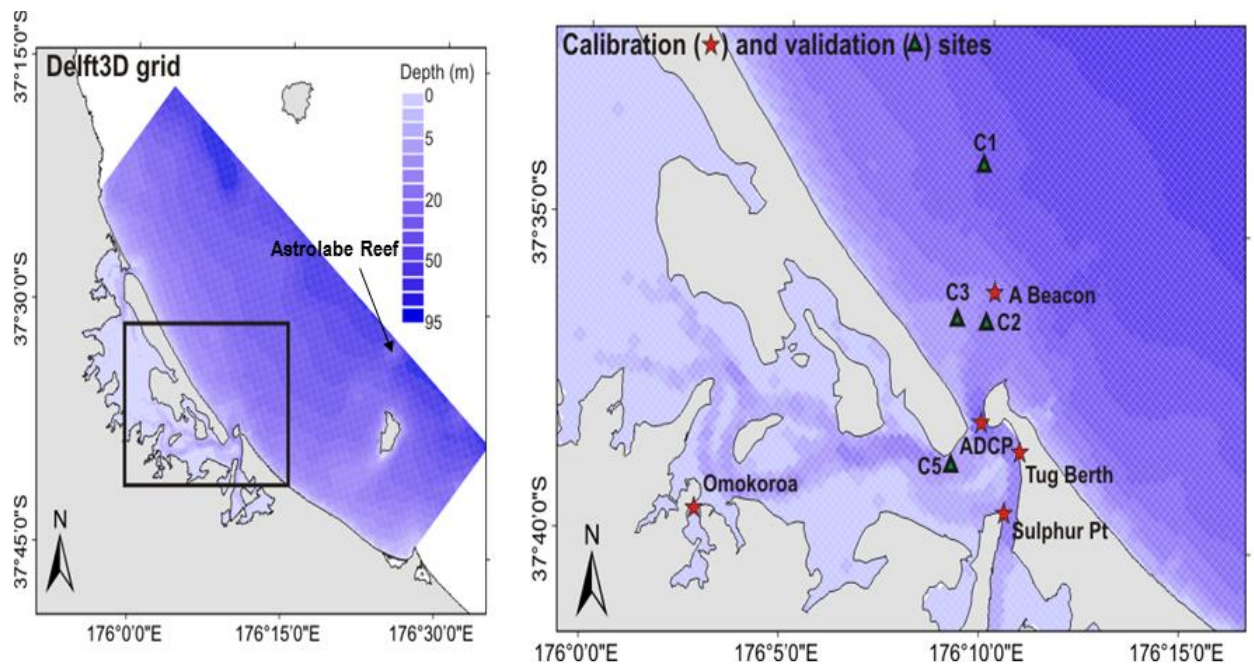


Figure 2: Delft3D model grid and location of calibration (red star) and validation (green triangle) sites.

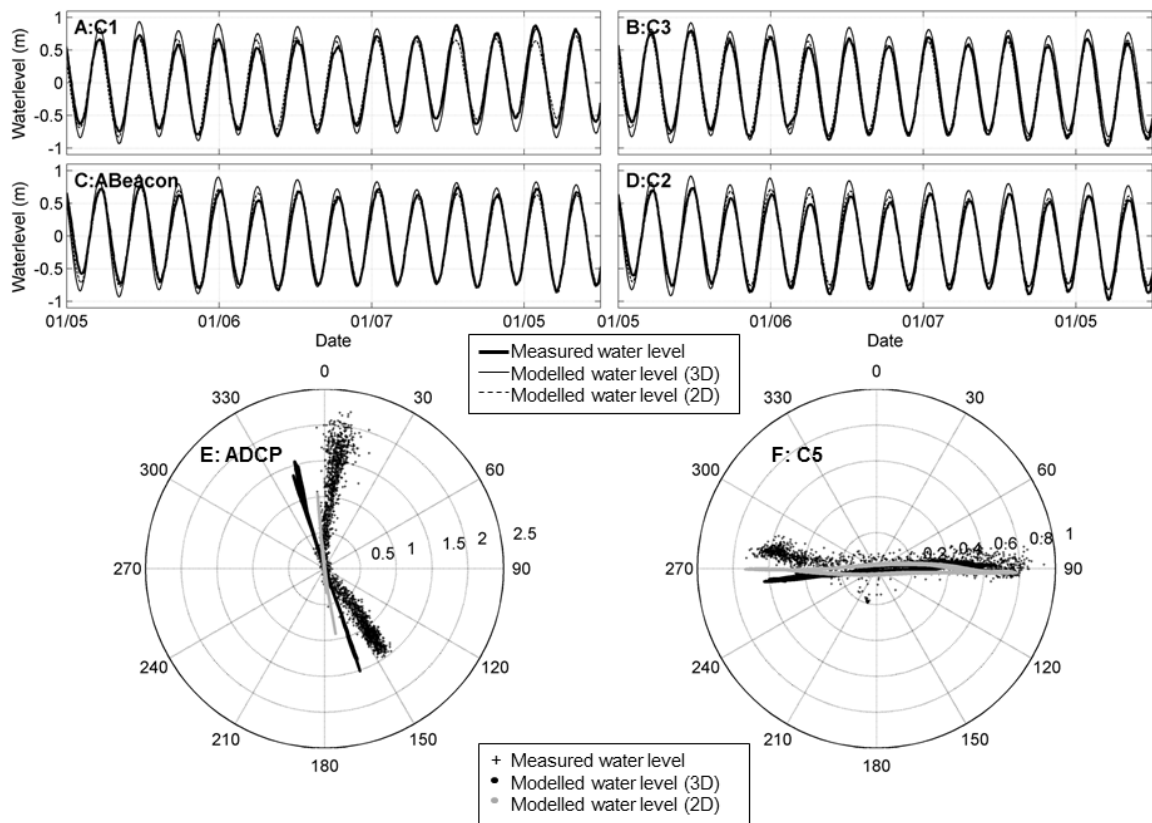


Figure 3: Measured and modelled water levels for validation sites C1 (A), C3(B), C2(D) and calibration site A Beacon (C), and measured and modelled current velocity and direction for the calibration ADCP site (E) and validation site C5 (F).

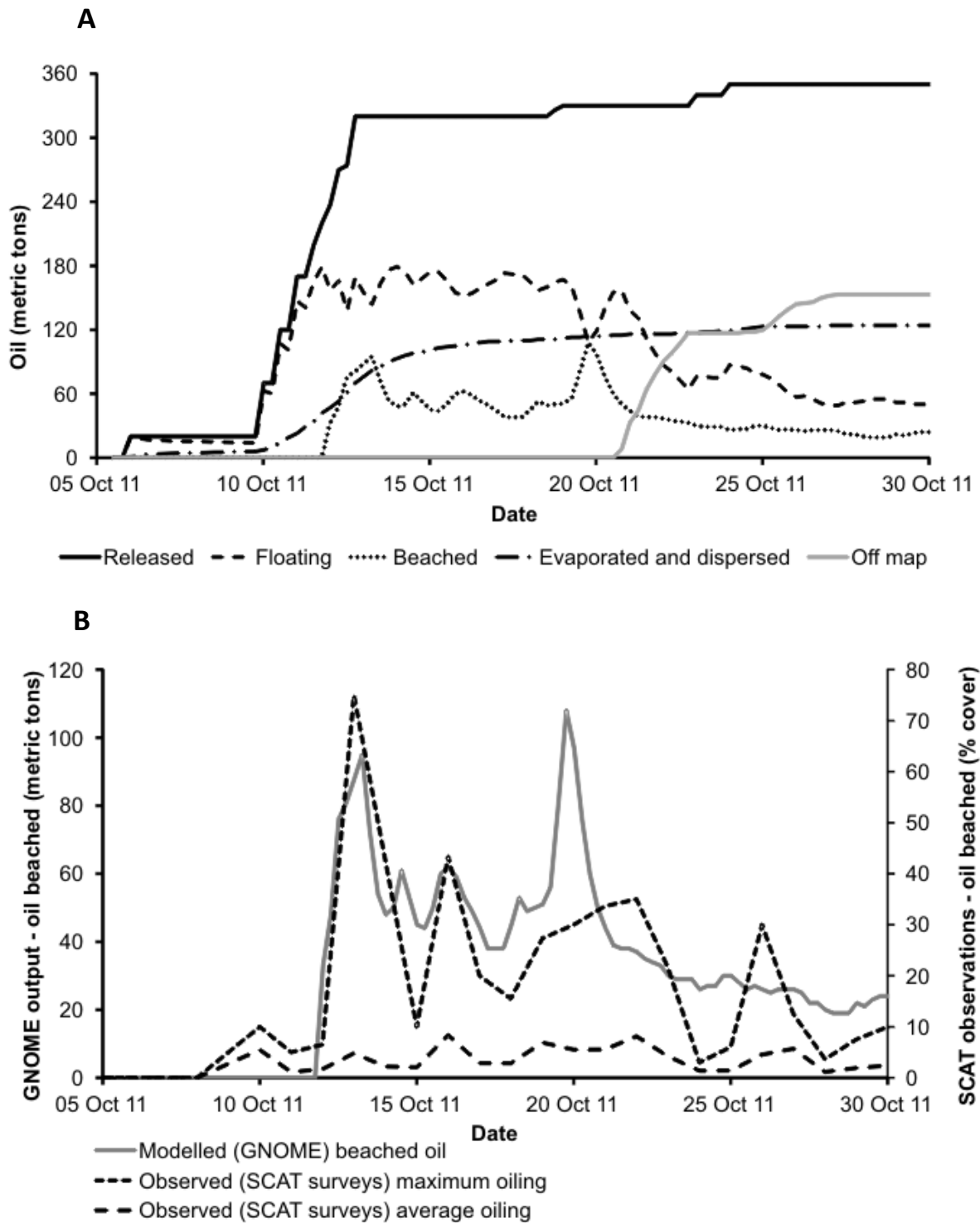


Figure 4: Panel A: Amount of oil released from the Rena, floating, beached on the shoreline, evaporated and dispersed or “off map” (i.e. outside of modelled area) throughout the duration of the GNOME simulation (5th October – 30th October 2011). Panel B: Modelled (GNOME) oil beached on the shoreline (in metric tons) and maximum and average oil percentage coverage as assessed by SCAT surveys.

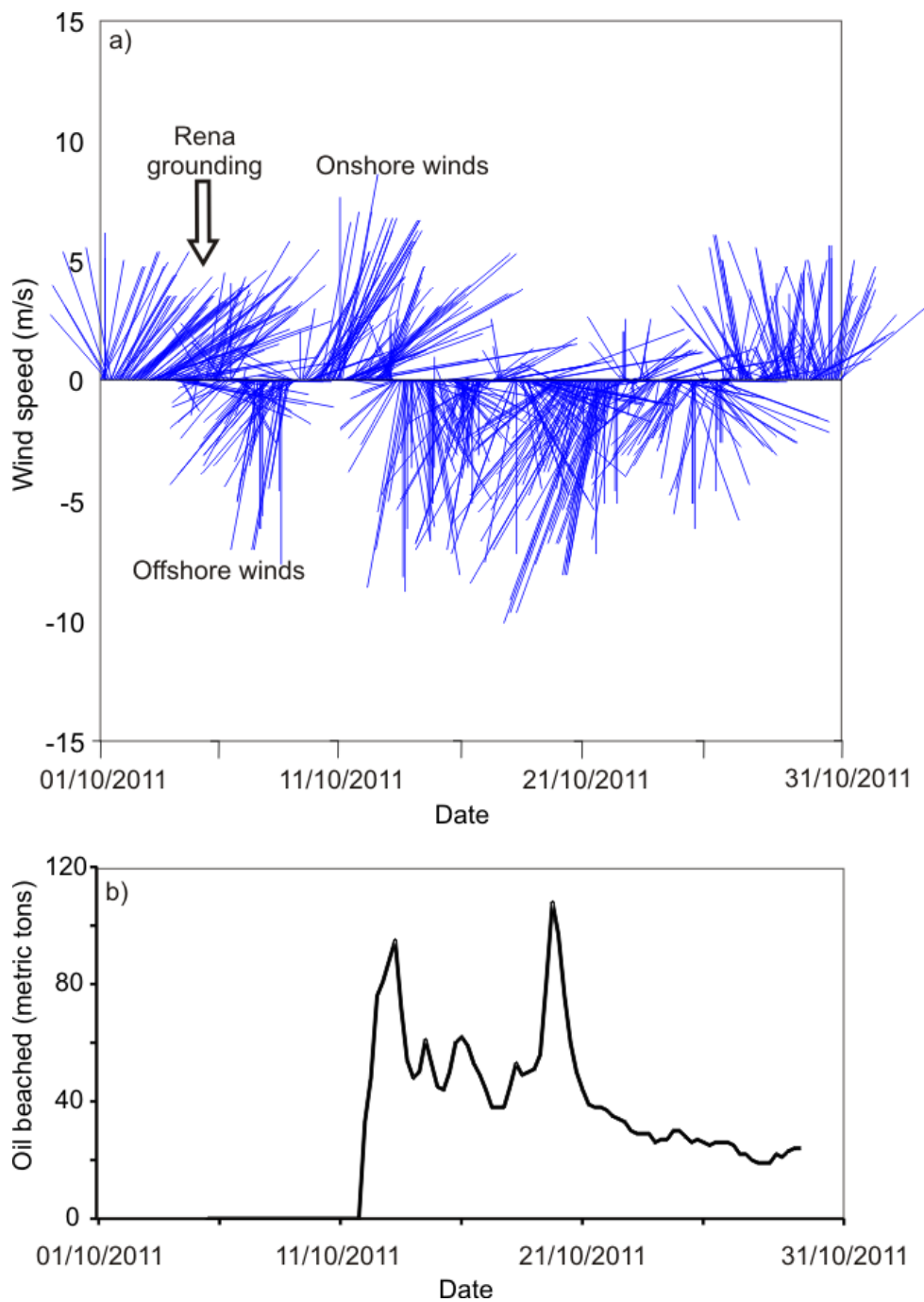


Figure 5: (a) Wind speed and direction measured at Tauranga airport in October 2011, with time of Rena grounding indicated by the arrow. Positive values on y axis represent northerly winds, negative values represent southerly winds. For example, offshore (southerly to south-westerly) winds are evident from 6th to 8th October 2011. (b) Modelled (GNOME) amount of oil beached on shoreline. Note peak in oil beached on shoreline 12th to 13th October after a period of onshore (north-easterly) winds, followed by a reduction in oil beached after moderate (> 5 m/s) offshore (southerly) winds.

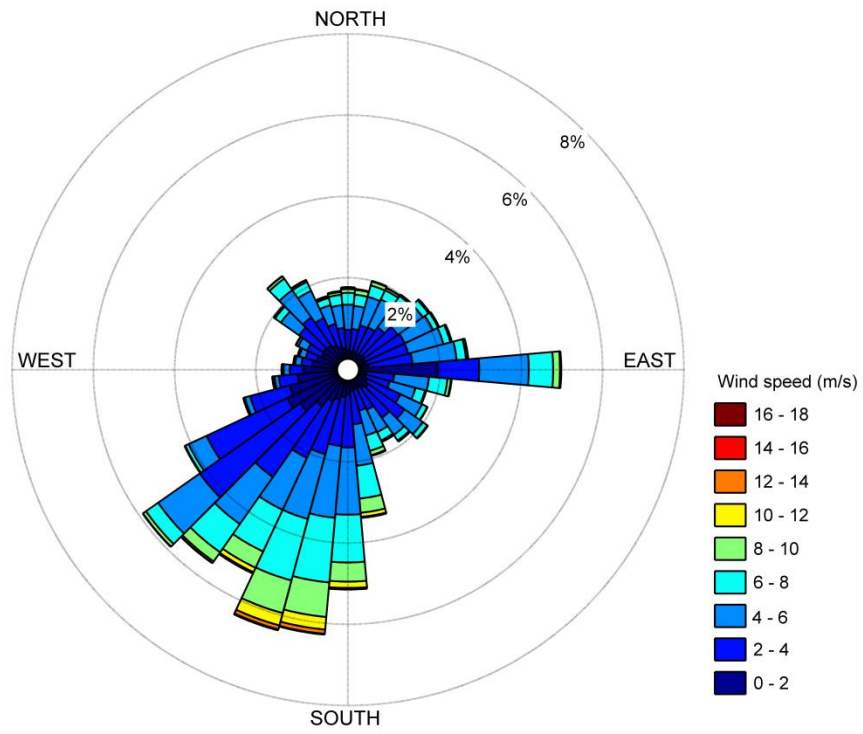


Figure 6: Wind speeds and directions measured at Tauranga Airport from 1995 to 2012. The colorbar is wind speed and the length of each radial bar reflects the probability of that wind condition occurring.

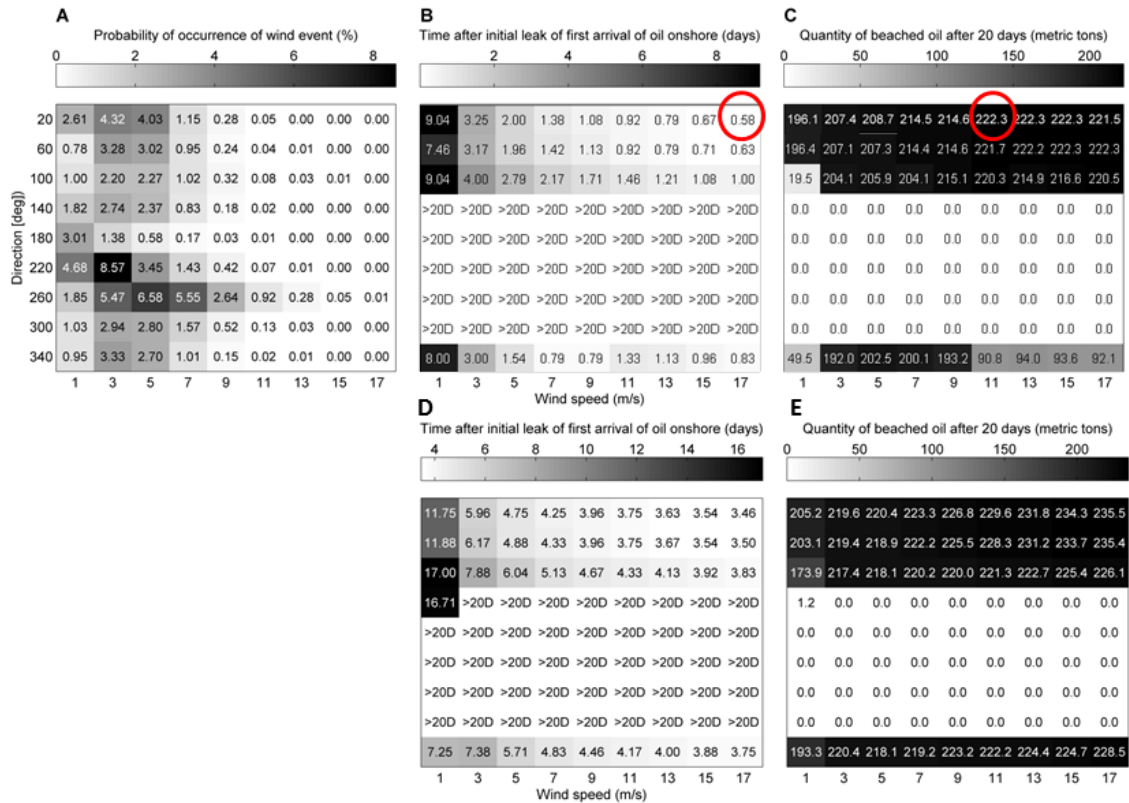


Figure 7: (A) The proportion of wind speeds and directions measured at Tauranga airport from 1995 to 2012, split into 81 wind events. (B) Modelled (GNOME) times after the initial oil leak for the first oil to be beached, for constant wind conditions. Simulations with no oil landing onshore within 20 days are labelled '>20D'. (C) Modelled (GNOME) quantities of oil beached at twenty days after the initial oil leak, for constant wind conditions. Circled in red are scenarios with (A) the most common wind condition, (B) the shortest time of arrival, and (C) the largest quantity of beached oil. Maps of the circled scenarios in Panels B and C are shown in Figure 8. Panels D and E are for the same wind conditions as in panels B and C, but have been modelled without including the effect of tides.

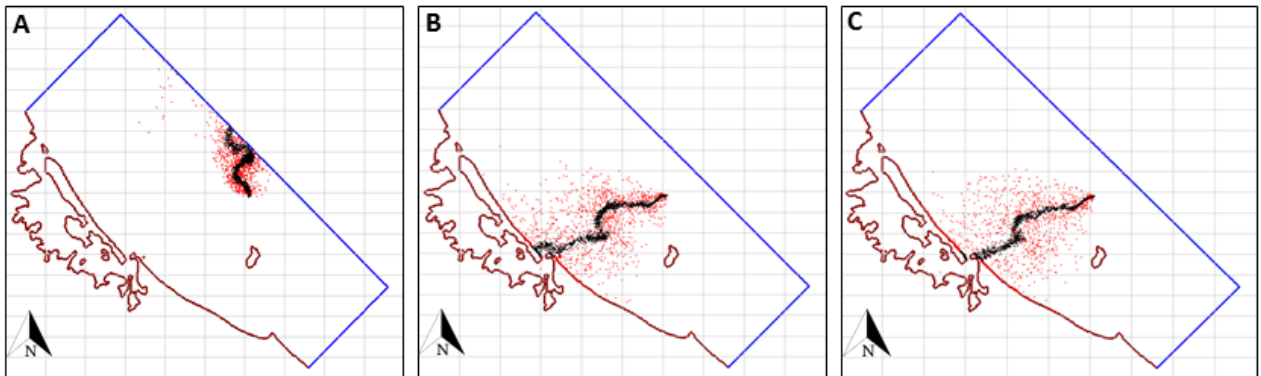


Figure 8: Maps of modelled (GNOME) oil plumes on 11th October at 9:20pm NZST, six days after the initial oil leak began, for (A) recorded wind conditions, (B) shortest time elapsed for first beaching of oil, and (C) largest quantity of beached oil after twenty days. Black dots represent the best guess location of oil particles, while red dots represent the minimum regret positions of oil particles.

Table 1: Calibrated model parameters for the Delft3D models.

Parameter	Value	Units
Threshold depth	0.01	m
Horizontal eddy viscosity	10	$\text{m}^2 \text{s}^{-1}$
Vertical eddy viscosity	0	$\text{m}^2 \text{s}^{-1}$
Turbulence model	k- ϵ	
Number of layers (3D)	16	
Number of layers (2D)	1	
Chézy roughness coefficient (3D)	Spatially variable (80 – 40)	$\text{m}^{1/2} \text{s}^{-1}$
Chézy roughness coefficient (2D)	Spatially variable (180 – 10)	$\text{m}^{1/2} \text{s}^{-1}$

Table 2: Calibrated model parameters for the GNOME model

Parameter	Value	Units
Diffusion	1	$\text{m}^2 \text{s}^{-1}$
Diffusion uncertainty	1	
Refloat half-life	12	Hours
Time step	0.17	Hours
Windage	1-4	%
Wind speed scale	2	m s^{-1}
Wind angle scale	0.4	Radians
Along current uncertainty	25	%
Cross current uncertainty	25	%

ii

Table A1.1: Statistical comparison of measured and Delft3D modelled water levels, tidal amplitude and phase. R^2 is the coefficient of determination, and MAE is the mean absolute error.

Site	Calibration or Validation	Water levels											
		R^2	MAE (m)	M2 amp error (m)	M2 phase error (deg)	N2 amp error (m)	N2 phase error (deg)	S2 amp error (m)	S2 phase error (deg)	K1 amp error (m)	K1 phase error (deg)	O1 amp error (m)	O1 phase error (deg)
A Beacon	Calibration	0.982	0.072	-0.01	-1.42	-0.01	1.29	0.01	4.77	-0.01	3.67	-0.01	8.26
Tug Berth	Calibration	0.971	0.078	0.03	-5.64	0.01	-3.69	0.02	1.19	-0.01	0.39	-0.01	9.93
Sulphur Point	Calibration	0.974	0.082	-0.01	-4.53	-0.01	-3.82	0.03	-1.24	-0.01	-15.46	0.01	2.89
Omokoroa	Calibration	0.965	0.082	-0.01	-6.73	-0.01	-6.56	0.03	-6.36	-0.01	-14.68	0.01	17.02
C1	Validation	0.968	0.077	-0.04	-4.23	0.01	1.95	0.03	-0.28	-0.02	-11.77	0.01	13.48
C2	Validation	0.965	0.078	-0.03	-3.89	0.02	2.45	0.03	0.79	-0.02	-13.48	0.01	15.23
C3	Validation	0.965	0.077	-0.02	-4.25	0.02	1.91	0.03	-0.37	-0.02	-13.61	0.01	16.54
C5	Validation	0.958	0.082	0.00	-6.20	0.03	1.34	0.03	-2.45	-0.02	-14.42	0.01	16.61

Table A1.2: Statistical comparison of measured and modelled (Delft3D) current speed and direction. MAE is the mean absolute error, Mean_{obs} is the mean of the measurements and Mean_{mod} is the mean of the model output.

Site	Calibration or Validation	Tide	Speed (m s ⁻¹)			Direction (degrees)		
			Mean _{obs}	Mean _{mod}	MAE	Mean _{obs}	Mean _{mod}	MAE
ADCP	Calibration	Total	1.10	0.72	0.41			
		Flood	1.10	0.72	0.33	145.77	163.88	18.11
		Ebb	1.48	0.85	0.61	8.00	337.19	30.48
C1	Validation	Total	0.06	0.02	0.04			
		Flood	0.05	0.02	0.04	240.41	239.51	13.70
		Ebb	0.02	0.02	0.01	66.28	64.48	9.13
C2	Validation	Total	0.19	0.10	0.10			
		Flood	0.12	0.07	0.06	213.19	205.17	13.31
		Ebb	0.29	0.14	0.22	20.71	21.33	11.17
C3	Validation	Total	0.16	0.06	0.10			
		Flood	0.12	0.06	0.05	178.40	174.57	13.02
		Ebb	0.23	0.09	0.21	334.05	335.48	10.86
C5	Validation	Total	0.45	0.41	0.10			
		Flood	0.47	0.35	0.10	278.54	265.47	12.82
		Ebb	0.55	0.50	0.08	88.02	87.11	3.52